AGU PUBLICATIONS

JGR

Journal of Geophysical Research: Biogeosciences

RESEARCH ARTICLE
10.1002/2017JG003796

Key Points:
- Soil microbes regulate decomposition but are rarely included in terrestrial biosphere models
- Here we develop a parsimonious and modular microbial physiology model that simulates carbon and nitrogen cycling in soils
- The model uses chemical, kinetic, and physical principles to estimate temperature, oxygen, and diffusion constraints on soil decomposition

Supporting Information:
- Supporting Information S1

Correspondence to:
A. C. Finzi,
afinzi@bu.edu

Citation:
Abramoff, R. Z., E. A. Davidson, and A. C. Finzi (2017), A parsimonious modular approach to building a mechanistic belowground carbon and nitrogen model, *J. Geophys. Res. Biogeosci.*, *122*, 2418–2434, doi:10.1002/2017JG003796.

Received 2 FEB 2017
Accepted 18 AUG 2017
Accepted article online 25 AUG 2017
Published online 21 SEP 2017

A parsimonious modular approach to building a mechanistic belowground carbon and nitrogen model

Rose Z. Abramoff[1,2], Eric A. Davidson[3], and Adrien C. Finzi[1]

[1]Department of Biology and PhD Program in Biogeoscience, Boston University, Boston, Massachusetts, USA, [2]Climate Sciences Department, Climate and Ecosystem Sciences Division, Lawrence Berkeley National Laboratory, Berkeley, California, USA, [3]Appalachian Laboratory, University of Maryland Center for Environmental Sciences, Frostburg, Maryland, USA

Abstract Soil decomposition models range from simple empirical functions to those that represent physical, chemical, and biological processes. Here we develop a parsimonious, modular C and N cycle model, the Dual Arrhenius Michaelis-Menten-Microbial Carbon and Nitrogen Phyisology (DAMM-MCNiP), that generates testable hypotheses regarding the effect of temperature, moisture, and substrate supply on C and N cycling. We compared this model to DAMM alone and an empirical model of heterotrophic respiration based on Harvard Forest data. We show that while different model structures explain similar amounts of variation in respiration, they differ in their ability to infer processes that affect C flux. We applied DAMM-MCNiP to explain an observed seasonal hysteresis in the relationship between respiration and temperature and show using an exudation simulation that the strength of the priming effect depended on the stoichiometry of the inputs. Low C:N inputs stimulated priming of soil organic matter decomposition, but high C:N inputs were preferentially utilized by microbes as a C source with limited priming. The simplicity of DAMM-MCNiP's simultaneous representations of temperature, moisture, substrate supply, enzyme activity, and microbial growth processes is unique among microbial physiology models and is sufficiently parsimonious that it could be incorporated into larger-scale models of C and N cycling.

Plain Language Summary Microorganisms that grow in the soil, like bacteria and fungi, affect how much carbon resides in the soil and how much is released to the atmosphere as CO_2. Mathematical models used to make climate change predictions often struggle to capture the activity of soil microbes in realistic ways. This study uses well-established descriptions of water and temperature effects on soil microbes to predict rate of carbon and nitrogen cycling in the soil. Our new model reproduces the changing relationship between temperature and microbial respiration during the growing season. We also show using a theoretical addition of root secretions that the microbial response depends on the nitrogen content of the added plant material. This model is simple and based on well defined physical and biological properties, and could be developed to model microbial activity at larger scales.

1. Introduction

Soil microorganisms cycle C and N through the biosphere [*Schlesinger*, 2005], incorporating these elements into cellular materials that are eventually mineralized into carbon dioxide (CO_2) and inorganic nitrogen (N). Soil is the largest terrestrial carbon (C) pool, and the flux of CO_2 from the soil to the atmosphere is dominated by microbial decomposition [*Schlesinger and Bernhardt*, 2013]. Hence, the rate of C mineralized by soil microorganisms affects the global C cycle.

The rate of C and N mineralization is often correlated with changes in temperature and precipitation, and from this relationship one can construct an empirical function between soil temperature, moisture, and mineralization rates [*Stanford et al*., 1973; *Stanford and Epstein*, 1974; *Rodrigo et al*., 1997]. Empirical soil temperature and moisture functions are used in terrestrial biosphere models for the purpose of projecting future mineralization rates under global change scenarios [*Coleman and Jenkinson*, 1996; *Parton et al*., 1987]. The temperature sensitivity of soil organic matter (SOM) depolymerization conforms to Arrhenius kinetics [*Lloyd and Taylor*, 1994]. However, soil temperature is not always the dominant driver of microbial activity, especially when substrate supply is limiting. When aerobic heterotrophs have limited access to C

monomers, either due to diffusion limitation or lack of oxygen (O_2), then alternative kinetics of substrate and/or enzyme concentration may better constrain mineralization rates (e.g., Michaelis-Menten, Reverse Michaelis-Menten, and equilibrium chemistry approximation) [*Tang*, 2015].

Despite well-known effects of temperature and substrate supply on the activity of soil microbes, microbial processes themselves are rarely explicitly included in terrestrial biosphere models. In these models, decomposition rate is determined using a rate constant that may vary as a function of soil temperature or moisture [*Jenkinson et al*., 1990; *Bolker et al*., 1998]. Indeed, none of the models in the Fifth Coupled Model Intercomparison Project (CMIP5) have process level representation of microbial physiology [*Todd-Brown et al*., 2013]. Where they have been included, the models suggest that representing microbes may improve predictions of soil C storage at the global scale [*Wieder et al*., 2013; *Hararuk et al*., 2015].

There are a number of theoretical microbial models that are candidates for scaling to ecosystem and global applications [*Wieder et al*., 2014, 2015], either by direct incorporation or by representing relevant mechanisms using simplified relationships (in the sense of *Xu et al*. [2014]). These models vary widely in complexity (Table S1 in the supporting information). Some models include explicit decomposition, uptake, and construction of degradative enzymes [*Schimel and Weintraub*, 2003; *Allison et al*., 2010; *He et al*., 2015; *Tang and Riley*, 2015], while others assume that decomposition rate is a function of microbial biomass [*Ahrens et al*., 2015] or that decomposition and uptake rates are identical [*German et al*., 2012; *Sulman et al*., 2014; *Wieder et al*., 2015]. Some focus only on temperature as the driver of decomposition kinetics, while others include substrate supply [*Tang and Riley*, 2015] or diffusion limitation on substrate availability [*Davidson et al*., 2012; *Manzoni et al*., 2014].

Many soil decomposition models ignore the role of N in regulating C mineralization and vice versa [*Moorcroft et al*., 2001; *Lawrence et al*., 2009; *Shevliakova et al*., 2009], instead using soil N concentration to modify mineralization rates [*Grant et al*., 1993; *Manzoni and Porporato*, 2009], using C quality as a proxy for N limitation (but see *Moorhead and Sinsabaugh* [2006] and *Sistla et al*. [2014]) or omitting the N cycle entirely [*Allison et al*., 2010; *Wang et al*., 2013; *Sulman et al*., 2014]. Microbes utilize C and N in plant litter and root exudates, as well as free monomers that have been cleaved from polymeric soil organic matter by extracellular enzymes [*Brzostek and Finzi*, 2011; *Frey et al*., 2013]. Plant input and soil organic matter C-to-N ratios (C:N) range from 25 to 300+ and 10 to 30+, respectively, and are usually significantly higher than that of microbial biomass (5–17) and extracellular enzymes (~3) [*McGroddy et al*., 2004; *Wallenstein et al*., 2006; *Cleveland and Liptzin*, 2007; *Brzostek and Finzi*, 2011; *Weintraub et al*., 2012]. As a result, microbial populations are often N limited, especially in organic, surface soils [*Mooshammer et al*., 2014]. This may explain why an increase in C-rich plant inputs can induce microbial population growth and nutrient limitation, which results in the production of extracellular enzymes that decompose SOM and thereby release mineralized N (i.e., priming) [*Brzostek et al*., 2013; *Kuzyakov*, 2010].

Stoichiometric constraints on decomposition are understood to be important to biogeochemical cycles at seasonal-to-decadal time scales [e.g., *Drake et al*., 2013; *Finzi et al*., 2011]. It is not clear, however, whether these constraints are necessary for accurate predictions of changes in SOM stocks and soil respiration. Simple empirical models may be sufficient to gap fill or make projections based on previously observed correlations, where predicted values remain within the ranges of values used to generate the correlation. In contrast, the goal of many models, especially microbial explicit models, is hypothesis testing and process level understanding [e.g., *Schimel and Weintraub*, 2003; *Allison et al*., 2010], especially when interactions of driving variables are not fully understood or where the model needs to be applied outside of a range of previous observations, as may be the case for sustained climate change and N deposition. In such cases, additional model complexity may be warranted to test and generate hypotheses about C and N cycling and to guide future research priorities.

In this paper, we develop a model of soil biogeochemistry that couples the C and the N cycles and represents microbial population growth and allocation to enzymes, DAMM-MCNiP. We tested the model's ability to predict heterotrophic soil respiration measurements in a midlatitude forest located in central Massachusetts, USA, compared to DAMM alone and a simple Arrhenius temperature model. We used a theoretical plant input addition experiment to demonstrate DAMM-MCNiP's utility in exploring plausible microbial, enzymatic, and soil C and N responses to changes in substrate supply.

2. Methods

2.1. Data

To test model performance, we used measurements of soil temperature, moisture, and C efflux from a trenching experiment at Harvard Forest, MA. A trench was dug to 1 m depth around a 5 × 5 m area in November 2008 in a mixed hardwood stand at the Little Prospect Hill tract of Harvard Forest. Automated measurements of C efflux were collected from April to October 2009 [*Savage et al*., 2013]. We used C efflux from trenched plots as an estimate of heterotrophic respiration. This data set is described in greater detail in *Davidson et al*. [2012] and *Savage et al*. [2013].

Although trenching is a widely used technique for estimating heterotrophic respiration in soil [*Giasson et al*., 2013], the treatment changes the soil environment in a way that may cause systematic biases in respiration measurements. For example, soil moisture is generally higher in trenched plots due to a lack of transpiration from live plants, and decomposition of dead roots may increase the measured heterotrophic respiration [*Epron et al*., 1999]. These effects can persist many months after the trenching treatment, but other field techniques for measuring heterotrophic respiration either affect the soil environment in a similar way to trenching [*Högberg et al*., 2001] or use proxies to partition C sources [*Schuur and Trumbore*, 2006].

2.2. Model Descriptions

2.2.1. Arrhenius Model

The Arrhenius equation to estimate the rate of a reaction is a null model to the more process-based models DAMM and DAMM-MCNiP, described below [*Arrhenius*, 1889a, 1889b]. It serves as an analogue for the first-order relationships with temperature commonly used in terrestrial biosphere models, although the specific functional forms used in these models vary [*Parton et al*., 1987; *Jenkinson and Coleman*, 2008]. We fit an Arrhenius function to soil temperature to predict the C efflux, F_C,

$$F_C = \alpha \times e^{-Ea/RT} \tag{1}$$

where α is the preexponential constant (mg C cm^{-3} h^{-1}), T is soil temperature (K) at 10 cm depth, Ea is the activation energy (kJ/mol), and R is the universal gas constant (kJ mol^{-1} K^{-1}). This model is based on the assumption that temperature is the main effect on the depolymerization rate and that depolymerization is the rate-limiting process controlling C efflux.

2.2.2. Dual Arrhenius and Michaelis-Menten Model

The Dual Arrhenius and Michaelis-Menten Model (DAMM) simulates the effects of soil temperature, soil moisture, and substrate supply on soil organic matter (SOM) depolymerization. Depolymerization is affected by soil temperature according to Arrhenius kinetics. Soil water content modifies the supply of two substrates, oxygen and a generalized C-containing substrate, both of which affect depolymerization using a Michaelis-Menten (i.e., dual Monod) kinetic approximation,

$$\text{Depolymerization rate} = V_{\max_S} \times \frac{[S]}{kM_S + [S]} \times \frac{[O_2]}{kM_{O_2} + [O_2]} \tag{2}$$

$$V_{\max_S} = \alpha \times e^{-Ea/RT} \tag{3}$$

where V_{maxS} is the maximum reaction rate calculated using the Arrhenius equation as above (equation (1)), $[S]$ is the C substrate concentration, kM_S is the half-saturation constant for the C substrate, $[O_2]$ is the oxygen concentration, and kM_{O2} is the half-saturation constant for oxygen. Oxygen concentration limits the depolymerization rate when soil water content is high, and C substrate supply limits depolymerization when soil water content is low because the substrate cannot diffuse to the reaction site. A complete description of the model equations and default parameters are available in *Davidson et al*. [2012, 2014]. The default parameters in DAMM were fit using the C efflux data set described above (section 2.1).

2.2.3. DAMM and the Microbial Carbon and Nitrogen Physiology Model

The DAMM model was combined with a microbial explicit C and N-cycling model, appropriately named the Microbial Carbon and Nitrogen Physiology Model (MCNiP), described in *Finzi et al*. [2015]. The combined model tracks seven pools, soil organic C (SOC) and N (SON), dissolved organic C (DOC) and N (DON), microbial biomass C and N, and extracellular enzymes (Figure 1). The terms "DOM" (dissolved organic matter) and

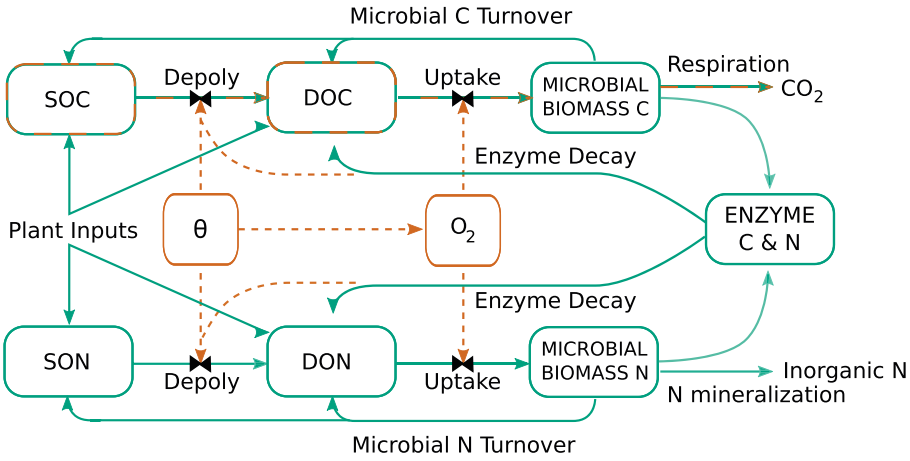

Figure 1. Conceptual model of DAMM-MCNiP. Orange boxes and arrows indicate components of the combined model that originate from DAMM, while green boxes and arrows indicate components originating from MCNiP. Striped orange and green boxes and arrows share components from both models. Solid lines indicate a transfer of mass, while dashed lines indicate an effect on a process rate. Depoly = depolymerization. θ = volumetric water content ($m^3\ m^{-3}$). Plant inputs refer to plant litter, which is partitioned to SOM and DOM_{CN} pools at each time step (h^{-1}). Root exudates enter the DOM_{CN} pool only.

"SOM" suggest that the former is in solution and the latter may or may not be soluble. In this model, we define DOM as monomeric and always in solution, while SOM is polymeric and can exist in both solid and aqueous phases (Texts S1 and S3). The combined model separates depolymerization from microbial uptake, and it allows feedback from C or N limitation of microbial processes to depolymerization via enzyme production. By combining DAMM and MCNiP into one model, it is possible to simulate the response of microbial activity to simultaneous changes in temperature, soil moisture, and substrate stoichiometry.

Soil temperature and moisture inputs constrain the rate of unprotected SOM depolymerization and uptake of dissolved organic matter C and N (DOM_{CN}) to the microbial biomass pool. The temperature sensitivity of SOM depolymerization to DOM_{CN} is controlled by Arrhenius kinetics. We modified the way that the supply of SOM and enzymes affect the depolymerization rate. In *Finzi et al.* [2015], MCNiP used forward Michaelis-Menten kinetics, but DAMM-MCNiP can have a very limited available substrate pool, especially when the soil is dry. As a result the enzyme and available substrate concentrations can be similar to each other, potentially violating the assumption of both forward Michaelis-Menten kinetics where available SOM ≫ enzyme concentrations, and reverse Michaelis-Menten kinetics where enzyme ≫ available SOM [*Wang and Post*, 2013]. Therefore, we use equilibrium approximation kinetics, a generalization of Michaelis-Menten kinetics for DAMM-MCNiP that makes no assumption about the relative size of the available SOM or enzyme pools,

$$\text{Depolymerization rate} = V_{\text{max}S} \times \frac{[\text{SOM}_{\text{avail}}] \times [\text{Enz}]}{kM_{\text{dep}} + [\text{SOM}_{\text{avail}}] + [\text{Enz}]} \tag{4}$$

$$V_{\text{max}_S} = \alpha_{\text{dep}} \times e^{-Ea_{\text{dep}}/\text{RT}} \tag{5}$$

where $V_{\text{max}S}$ is the maximum reaction rate determined using Arrhenius kinetics, $[\text{SOM}_{\text{avail}}]$ is the concentration of soluble, bio-available SOM (see Text S3, equation (S3)), [Enz] is the concentration of extracellular enzyme at the reaction site, and kM_{dep} is the half-saturation constant for enzymes. Microbial uptake of DOM_{CN} is limited by both DOM_{CN} concentration and oxygen concentration,

$$\text{Uptake rate} = V_{\text{max}D} \times \frac{[\text{DOM}_{\text{CN}}]}{kM_{\text{upt}} + [\text{DOM}_{\text{CN}}]} \times \frac{[\text{O}_2]}{kM_{\text{O}_2} + [\text{O}_2]} \tag{6}$$

$$V_{\text{max}_D} = \alpha_{\text{upt}} \times e^{-Ea_{\text{upt}}/\text{RT}} \tag{7}$$

where $V_{\text{max}D}$ is the maximum reaction rate, $[\text{DOM}_{\text{CN}}]$ is the concentration of DOM_{CN}, and kM_{upt} is the half-saturation constant for DOM_{CN}. C or N uptake is partitioned in the microbial pool to maintenance, growth,

and enzyme production. Enzyme production can be limited by either C or N according to Liebig's law of the minimum, consistent with the concept of overflow metabolism wherein excess C or N is mineralized after maintenance, enzyme production, and biomass growth (in the sense of *Schimel and Weintraub* [2003]),

$$\text{Enzyme production} = q \times \text{UPT}_\text{N} \quad [\text{N limited}] \tag{8}$$

$$\text{Enzyme production} = p \times (\text{CUE} \times \text{UPT}_\text{C})/\text{CN}_\text{E} \quad [\text{C limited}] \tag{9}$$

where q and p are partitioning coefficients, UPT_C and UPT_N are the C and N taken up in the current time step, CUE is carbon use efficiency, and CN_E is the C:N of enzymes. Inputs to the model include temperature, soil moisture, litter, and if rhizosphere, root exudate C and N. Outputs used in this study are the seven C and N pools as well as rates of C (i.e., C efflux) and N mineralization. For the purposes of this study we did not consider microbial immobilization of mineralized N. Litter is partitioned to SOM and DOM_CN pools at each time step (h^{-1}). Root exudates enter the DOM_CN pool only. Both DOM_CN inputs and the fraction of unprotected SOM follow a prescribed seasonality (Text S1) [*Farrar et al*., 2003; *Keiluweit et al*., 2015]. In all model simulations, we assumed an effective depth of 10 cm (in the sense of *Davidson et al*. [2012]).

Model parameters were identical to original DAMM and MCNiP parameters, except for the preexponential constant (α_dep), activation energy (Ea_dep), and half-saturation constant (Km_dep) for SOM depolymerization, and the preexponential constant (α_upt) and activation energy (Ea_upt) for DOC uptake. In DAMM, these parameters were fit to the validation data set, so in order to provide default parameters for DAMM-MCNiP we estimated α_dep, Ea_dep, α_upt, and Ea_upt from incubation measurements of mean β-glucosidase activity in organic and mineral soil [*Davidson et al*., 2012; *Finzi et al*., 2015]. The values for α_dep and Ea_dep were set to be identical to those for α_upt and Ea_upt, respectively, because we could not experimentally distinguish between depolymerization and uptake kinetics. The default value for the half-saturation constant, Km_dep, in DAMM-MCNiP was estimated such that at standard temperature, 293 K (20°C), and the mean soil moisture value for this site, 0.229 cm^3 H_2O cm^{-3} soil, Km_dep was equal to the initial available substrate SOM concentration (in the sense of *Davidson et al*. [2012]). In contrast to *Allison et al*. [2010], we did not choose a Km_dep larger than the available SOM pool. Microbes in MCNiP have access to the entire SOM pool, so using a Km_dep value that is high relative to the SOM pool size prevents substrate from saturating enzymes at the reaction site. However, microbes in DAMM-MCNiP do not have access to the entire SOM pool. Therefore, our parameterization of DAMM-MCNiP allows for substrate to saturate a reaction site, for example, if substrate is temporarily mobilized during a wet-up event [*Birch*, 1958; *Sierra et al*., 2015]. Additional comments on parameter value sources and complete equations for DAMM-MCNiP can be found in Texts S2 and S3, respectively [*Hopkinson et al*., 1997; *Neff and Hooper*, 2002; *Schimel and Weintraub*, 2003; *Allison et al*., 2010; *Davidson et al*., 2012; *Lemos*, 2013; *Averill*, 2014].

We spun up the model for 1000 years. DAMM-MCNiP pools update over time, so it was important that we simulate a full year of soil temperature and moisture data during spin-up. We reconstructed a full year of soil temperature measurements from growing season data using a linear fit to nearby Fisher Meterological Station at the Harvard Forest. Measurements of soil temperature were collected at 15 min intervals [*Boose and VanScoy*, 2015]. We fit hourly averaged soil temperature at 10 cm depth to measurements (described below; $R^2 = 0.86$, $P < 0.001$). We used this fit to estimate soil temperature at 10 cm depth at the Harvard Forest site for the remainder of the year (Figure S1a). For soil moisture measurements, we used 2010 measurements collected at 30 min intervals at the Harvard Forest Environmental Measurement Station tower [*Munger et al*., 2016].

2.3. Model Evaluation

We used C efflux data collected at the Harvard Forest to fit each of the three models—the Arrhenius model, DAMM alone, and DAMM-MCNiP. The Arrhenius model was fit to data using nonlinear least squares regression (function *nls*, package *stats*, R Version 3.2.0). DAMM parameter fitting was described in *Davidson et al*. [2012]. DAMM-MCNiP was fit to the data set by minimizing the residuals of the model using a Newton-type method (function *modFit*, method *Newton*, package *FME*, R Version 3.2.0; Table 1).

Linear regression was used to fit the output predicted by each model with C efflux measurements from trenching and to estimate the root-mean-square error (RMSE) of the model fit. We computed the correlation coefficient (Pearson's ρ) between model-predicted C efflux and soil temperature or soil moisture. We used the

Table 1. DAMM-MCNiP Model Parameter Abbreviations, Units, Default Values, and Values Fit to Data

Parameter	Units	Default Value	Fit Value	Description
Depth	cm	10	-	Depth assumption for all model pools
litterSOC	mg cm^{-3} h^{-1}	input	input	Litter input to SOC pool
litterDOC	mg cm^{-3} h^{-1}	input	input	Litter input to DOC pool
T	K	input	input	temperature in Kelvin
θ	cm^3 H_2O cm^{-3} soil	input	input	volumetric water content
BD	g cm^{-3}	0.80	0.76	bulk density
PD	g cm^{-3}	2.52	2.50	particle density
O_{2frac}[a]	L O_2 L^{-1} air	0.209	0.203	volume fraction of O_2 air
frac[a]	g C cm^3 g C cm^{-3}	4.14×10^{-4}	3.79×10^{-4}	fraction of unprotected SOM, using soluble substrate estimated from *Magill et al.* [2000]
dLiq[a]	-	3.17	3.14	diffusion coefficient for unprotected SOM and DO_{CN} in liquid
dGas[a]	-	1.67	1.63	diffusion coefficient for O_2 in air
kM_{O2}[a]	cm^3 O_2 cm^{-3} air	0.121	0.115	Half-saturation constant for O_2
R	kJ K^{-1} mol^{-1}	8.31×10^{-3}	8.31×10^{-3}	universal gas constant
p[a]	-	0.50	0.50	proportion of assimilated C allocated to enzyme production
q[a]	-	0.50	0.50	proportion of assimilated N allocated to enzyme production
a[a]	-	0.50	0.49	proportion of enzyme pool acting on SOC pool ($1 - a$ = proportion acting on SON pool)
initSOC	mg cm^{-3}	65.25	65.25	initial SOC pool
initSON	mg cm^{-3}	2.192	2.192	initial SON pool
initDOC	mg cm^{-3}	2.0×10^{-3}	2.0×10^{-3}	initial DOC pool
initDON	mg cm^{-3}	1.1×10^{-3}	1.1×10^{-3}	initial DON pool
initBiomassC	mg cm^{-3}	1.970	1.970	initial microbial biomass C
initBiomassN	mg cm^{-3}	0.197	0.197	initial microbial biomass N
refSOC	mg cm^{-3} h^{-1}	5.0×10^{-4}	5.0×10^{-4}	reference rate for input to SOC pool
ampSOC	mg cm^{-3} h^{-1}	5.0×10^{-4}	5.0×10^{-4}	amplitude of seasonal cycle for input to SOC pool
initEnz	mg cm^{-3}	0.0339	0.0339	initial enzyme pool
refDOC	mg cm^{-3} h^{-1}	5.0×10^{-4}	5.0×10^{-4}	reference rate for input to DOC pool
ampDOC	mg cm^{-3} h^{-1}	5.0×10^{-4}	5.0×10^{-4}	amplitude of seasonal cycle for input to DOC pool
r_{death}[a]	h^{-1}	1.5×10^{-4}	1.5×10^{-4}	microbial turnover rate
$r_{enzLoss}$[a]	h^{-1}	1.0×10^{-3}	1.0×10^{-3}	enzyme turnover rate
micToSom[a]	mg mg^{-1}	0.50	0.49	fraction of dead microbial biomass allocated to SOM
α_{dep}[a]	mg SOM cm^{-3} (mg Enz cm^{-3})$^{-1}$ h^{-1}	1.08×10^{11}	1.06×10^{11}	preexponential constant for SOM depolymerization
α_{upt}[a]	mg DOC cm^{-3} (mg biomass cm^{-3})$^{-1}$ h^{-1}	1.08×10^{11}	1.08×10^{11}	preexponential constant for DOC uptake
kM_{dep}[a]	mg cm^{-3}	0.0025	0.0025	Half-saturation constant for SOM depolymerization
kM_{upt}[a]	mg cm^{-3}	0.30	0.29	Half-saturation constant for DOC uptake
CUE[a]	mg mg^{-1}	0.31	0.30	Carbon use efficiency
Ea_{dep}[a]	kJ mol^{-1}	61.77	64.32	Ea for SOM depolymerization
Ea_{upt}[a]	kJ mol^{-1}	61.77	60.26	Ea for DOC uptake
CN_S	-	27.6	28.1	C:N of soil
CN_L	-	50.0	48.8	C:N of litter
CN_M	-	10.0	9.8	C:N of microbial biomass
CN_E	-	3.0	2.9	C:N of enzymes
CN_{EX}	-	27.6	28.1	C:N of root inputs

[a]Parameter values included in the sensitivity analysis.

ratio of $\rho_{temperature}$ to $\rho_{moisture}$ as an estimate of the sensitivity (ρ_{sens}) of modeled C efflux to temperature relative to soil moisture,

$$\rho_{sens} = \rho_{temperature} / \rho_{moisture} \quad (10)$$

Values greater than 1 indicate that C efflux is more correlated with temperature than with soil moisture.

2.4. Sensitivity Analyses for DAMM-MCNiP

In order to partition the relative contribution of temperature, soil moisture, and plant inputs to explaining variation in SOC pool size, we ran 125 model realizations ranging from −5°C to +5°C change from control run temperature, and from 10% to 200% of default soil moisture and plant input values (Table S2). We built a normalized regression relationship between SOC and temperature, soil moisture, and plant inputs and

calculated the partial R^2 for each term (functions *scale*, *lm.beta*, *partial.R2*; packages *lm.beta*, *asbio*; R Version 3.2.0). All analyses were conducted in R Statistical Software (R Development Core Team, 2013).

We conducted a global variance-based sensitivity analysis in order to calculate the sensitivity of C efflux to 18 of the parameter values listed in Table 1. We calculated a first-order sensitivity index that is bound between 0 and 1,

$$S_i = \frac{\mathrm{VAR}_{p_i}\left(E_{p_{\sim i}}(Y|p_i)\right)}{\mathrm{VAR}(Y)} \tag{11}$$

where p_i is the ith parameter, $p_{\sim i}$ are all parameters that are not the ith parameter, VAR is the variance, and E is the expectation [*Saltelli et al*., 2010]. For each parameter, we sampled across a range of the parameter's default value ±10% with 60,000 model evaluations following the Sobol sampling method [*Saltelli et al*., 2008]. We performed this analysis in *Matlab* [2017], using the toolbox SAFE R1.1 [*Pianosi et al*., 2015].

Collinearity refers to correlation between two or more variables, traditionally in a linear regression. In a numerical model, high collinearity makes it difficult to fit parameters because two or more parameters may trade off with each other, resulting in many combinations of parameter values with equal model fit. To determine whether there is collinearity among the parameters in the DAMM-MCNiP model, we performed a parameter identifiability test that estimates a collinearity index for the fitted parameters (function *collin*, package *FME*, R Version 3.2.0). The collinearity index, γ, is an estimate of linear dependence, with a lower bound of 1 when all terms are orthogonal and an upper bound of infinity when all terms are linearly dependent. The most useful interpretation of γ is that a change in one parameter can be compensated by a $1 - 1/\gamma$ change in other parameters, so at $\gamma = 20$, 95% of the effect of a change in one parameter can be compensated by modifying the values of other parameters, thereby limiting the identifiability of the model parameters [*Brun et al*., 2001; *Omlin et al*., 2001].

2.5. Double Input Experiment With DAMM-MCNiP

We simulated three input scenarios where C and N were added in varying amounts and with different stoichiometry to study changes in soil C and N pools. These scenarios are analogous to plant input manipulations or as a result of root exudation. To isolate the effect of stoichiometry on soil C and N pools, we ran the model with constant soil temperature and moisture using default parameter values. Each simulation ran for 190 days with 0.96 gC m^{-2} d^{-1} of plant input, about 2.4 gC/kg soil (0.96 gC/m^2 d × 190 days ÷ 76 kg soil/m^2 bulk density), within the range of other priming studies [*Fontaine et al*., 2004; *Graaff et al*., 2010]. Litter inputs to the SOM pool and root exudate inputs to the DOM pool had a C:N of 50 [*Abramoff and Finzi*, 2016] and 27.6 (Text S2), respectively. On day 95, we added double C inputs (C:N of 55.2), double N inputs (C:N of 13.8), or both (C:N of 27.6) to the DOM pool. Although we applied the doubled C and N treatments as if they were a single element fertilization, from a microbial perspective, these treatments are identical to changing the stoichiometry of the incoming plant input. Therefore, one could also think of the treatments as C-rich inputs, N-rich inputs, and double inputs, respectively. A control run with no change to C and N inputs was used to normalize the C and N pools for comparison. We considered absolute changes in soil pools and fluxes as well as changes to the proportion of C efflux that is made up of decomposed SOC, analogous to priming experiments that partition C efflux into native and added C using enriched C isotope tracers [*Graaff et al*., 2010; *Hartley et al*., 2012; *Murphy et al*., 2015; *Wild et al*., 2016]. We tracked the fate of input DOM by verifying that changes to the microbial biomass and enzyme pools were small (<2% of initial value) such that at each time step, C efflux ≈ Inputs + SOC decomposition.

3. Results

3.1. Model Performance

From a visual inspection of the model output all three models captured the seasonality of C efflux well (Figure 2a). The Arrhenius model and DAMM predicted similar rates of C efflux, while DAMM-MCNiP predicted a slightly lower rate, especially during the shoulder seasons when there was lower input from litter decomposition. All three models explained 52–56% of the variation in the C efflux data and had little bias in the slope of the relationship between the predicted and measured C efflux (slope = 0.93–1.04; Figure 2b and S2).

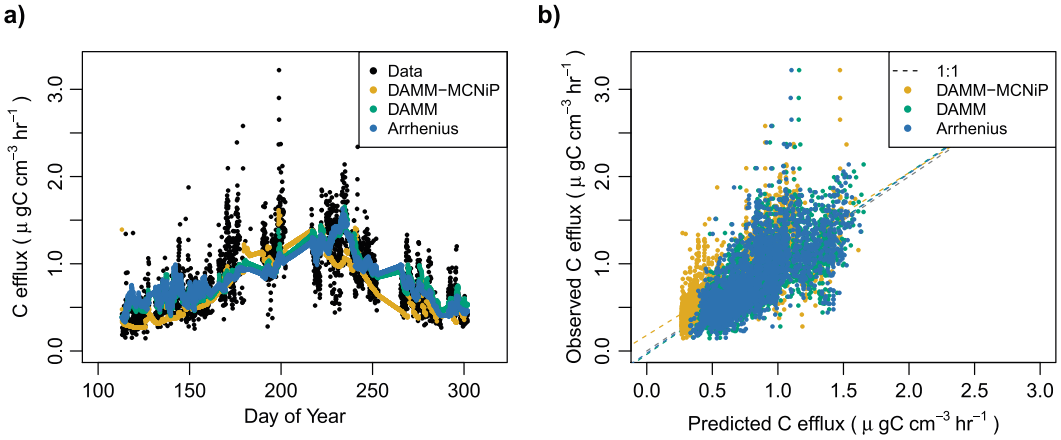

Figure 2. (a) Time series of observed (black symbols) and predicted (colored symbols) C efflux rate and (b) linear regression of observed and predicted C efflux rate using DAMM-MCNiP (slope = 0.93, R^2_{adj} = 0.56, and RMSE = 0.25), DAMM (slope = 1.04, R^2_{adj} = 0.55, and RMSE = 0.26), and Arrhenius (slope = 1.03, R^2_{adj} = 0.52, and RMSE = 0.27). The gray dashed line is the 1:1 line. Colored dashed lines are the regression fit for each model. RMSE is the root-mean-square error. All model fits were significant at the $P < 0.001$ level.

In all three models, the Pearson correlation coefficient (ρ) between model-predicted C efflux and soil temperature at 10 cm was on average ~4 times greater than that for soil moisture at 2–8 cm. The mean ρ for temperature was 0.91 (standard deviation = 0.10), and the mean ρ for moisture was 0.22 ± 0.2 (Table 2). The Arrhenius model was necessarily more sensitive to temperature than soil moisture (ρ_{sens} = 32) because soil moisture was not included in the function. DAMM alone was also more sensitive to temperature compared to soil moisture, with a ρ_{sens} of 4.6. Of the three models, DAMM-MCNiP was most sensitive to soil moisture (ρ_{sens} = 1.8), especially at shorter time scales. The correlation coefficient between DAMM-MCNiP and soil moisture was greater than 0.96 for three different 5 day periods spanning rain events (DOY 125–130, 197–202, and 240–245), compared to ρ = 0.43 for the whole growing season (Table 2). Further, the correlation coefficient between DAMM-MCNiP and soil moisture was greater over short compared to long time intervals regardless of whether or not a rain event was present (Figure S3).

Across model realizations of DAMM-MCNiP, temperature explained 23% of the variation in the SOC pool size after 1 year, while soil moisture and plant inputs explained 14% and 23%, respectively. The total variation in SOC explained by DAMM-MCNiP was 41% (SOC ~ temperature + poly(soil moisture) + inputs; $F_{4,120}$ = 22.87, $P < 0.0001$, and R^2_{adj} = 0.41). DAMM-MCNiP simulated a temperature hysteresis in the seasonal C efflux that matched the measured temperature hysteresis (Figures 3a and 3b). In contrast, the DAMM and Arrhenius models did not have a hysteresis between temperature and C efflux (Figures 3c and 3d). C efflux was elevated in the midgrowing season (DOY 150–200) relative to the fall (DOY 200–270).

3.2. Sensitivity Analyses for DAMM-MCNiP

A 5°C increase in soil temperature increased C efflux relative to ambient soil temperature by 73 gC m^{-2} over the growing season (gs^{-1}; pink symbols; Figure 4a). Similarly, a 50% decrease in soil moisture suppressed C efflux by 116 gC m^{-2} gs^{-1} (blue symbols; Figure 4a). C efflux was nonlinearly related to changes in both temperature and moisture. In particular, the effect of warming or drought increased over the growing season as the treatment persisted (Figure 4b). A 50% decrease in plant inputs caused a ~50% decrease in C efflux, summing to 148 gC m^{-2} gs^{-1}. In contrast to the warming and drought experiments, plant inputs were approximately linearly

Table 2. Pearson Correlation Coefficients Between Model-Predicted C Efflux and Soil Temperature or Soil Moisture in Each Year

	Soil Temperature (°C)	Soil Moisture (cm^3 H_2O cm^{-3} soil)
DAMM-MCNiP	0.80	0.43
DAMM	0.96	0.21
Arrhenius	0.99	0.03
2009 Data	0.82	0.24

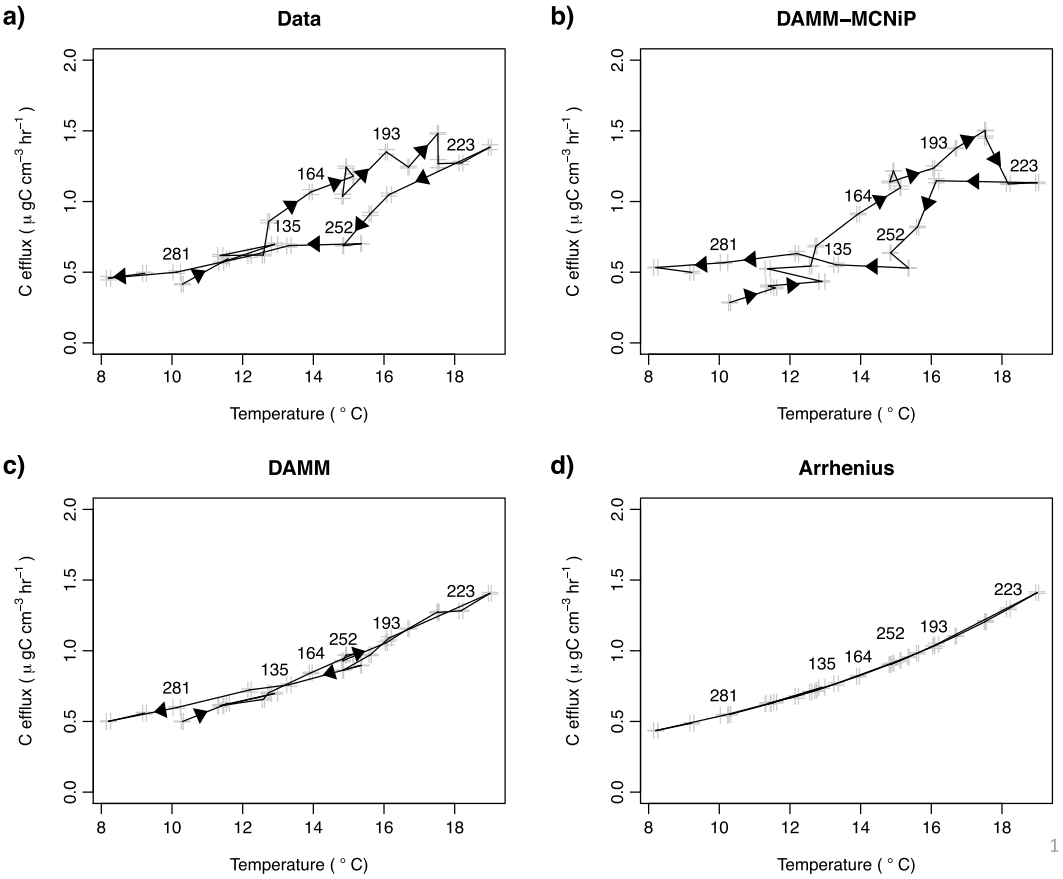

Figure 3. Weekly average C efflux rate plotted against temperature during (a) the 2009 growing season at the Harvard Forest trenched plots ("Data"), (b) DAMM-MCNiP-simulated bulk soil ("DAMM-MCNiP"), (c) DAMM-simulated bulk soil ("DAMM"), and (d) predictions from the Arrhenius model ("Arrhenius"). The text indicates the day of year (DOY), and the arrowheads indicate the transition from the start (DOY 113) to the end (DOY 303) of the growing season. The gray lines behind each point are the standard error of the mean.

related to C efflux (yellow symbols; Figure 4b). Warming and plant input removal resulted in an SOC decline of about 1% over the growing season, while drought resulted in ~2% increase in the SOC pool (Figure 4c).

Of the parameters included in the global, variance-based sensitivity analysis, activation energy of depolymerization (Ea_{dep}) was by far the most sensitive parameter (Figure S4a), followed by the activation energy of uptake (Ea_{upt}) when Ea_{dep} was excluded from the analysis (Figure S4b). The preexponential constant for decomposition (α_{dep}), liquid diffusivity (dLiq), and the average fraction of SOM that is not chemically or physically protected (refFrac) also had a sensitivity index greater than 0.2. The activation energy of depolymerization determined by the model fit to trenching data was 64 kJ mol^{-1}. The activation energy of uptake was estimated to be 60 kJ mol^{-1}.

Parameter collinearity is not commonly reported, but was relatively low for DAMM-MCNiP (Figure S5) compared to two simple four- and five-parameter models with collinearity indices of 59 and 19,487,389, respectively [*Brun et al.*, 2001; *Soetaert*, 2016]. Even with all 26 parameters included, the collinearity index for DAMM-MCNiP never exceeded 45.

3.3. Double Input Experiment With DAMM-MCNiP

Doubling root C input immediately increased the DOC pool size and efflux rate by 40–80%. Both increased nonlinearly with respect to microbial biomass C and N (Figure 5a). Microbial biomass production increased linearly with C addition. Doubling root C input increased uptake of DON, and the size of this pool decreased as a result. Despite the large increase in C efflux, no additional SOC was decomposed (Figure 5d) and as a result the proportion of C efflux made up of decomposed SOC declined from 41% to 30% after C addition.

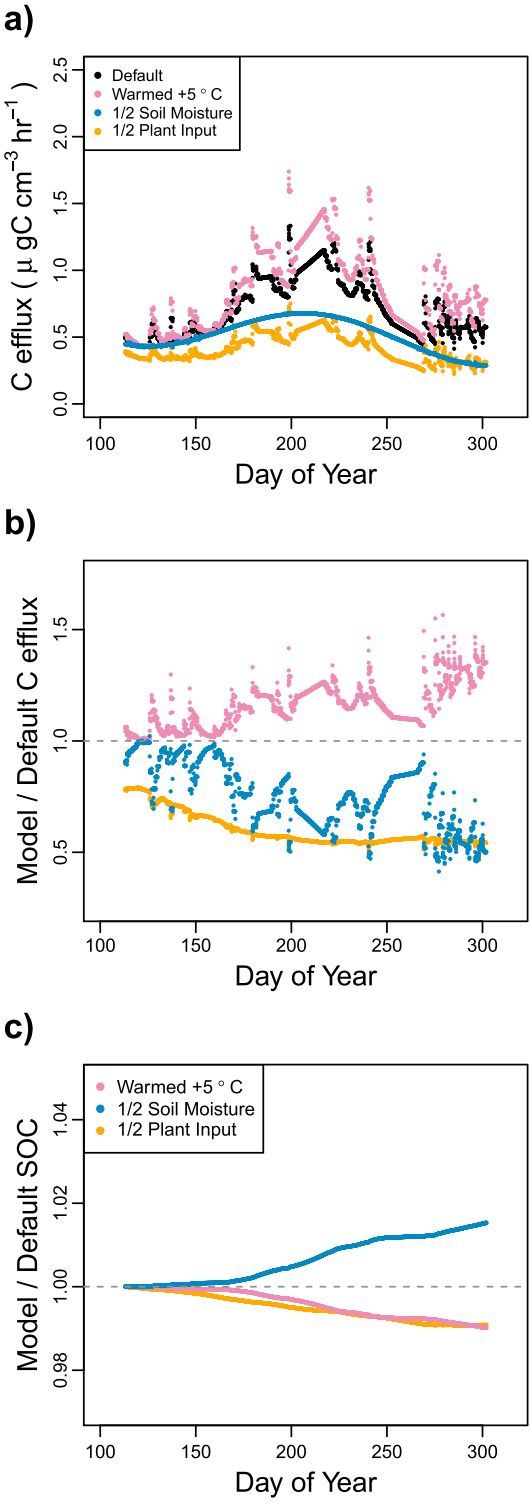

Figure 4. (a) Model-predicted C efflux rate using default forcings (black symbols), +5°C temperature increase (pink symbols), 50% of default soil moisture (blue symbols), and 50% of default plant inputs (yellow symbols). (b) Ratio between model-predicted C efflux for each of the three model scenarios and the default scenario. The horizontal gray dashed line is unity. (c) Ratio between model-predicted SOC for each of the three model scenarios and the default scenario.

When N inputs were doubled, there was a large, nonlinear increase in total enzyme production as an apparent N limitation of enzyme production was relieved, and the DON pool increased by ~60%. There was, however, a decrease in microbial biomass and only a small stimulation of C efflux (Figure 5b). SOC decomposition increased by ~3% (Figure 5d, dash line), and as a result the proportion of C efflux made up of decomposed SOC increased from 41% to 45%.

Doubling C and N inputs together resulted in an additive increase in C efflux, microbial biomass, and dissolved C and N pools. There was a nonadditive and sustained increase in enzyme production throughout the growing season, in contrast to the leveling off of enzyme production at day of year ~280 in the doubled N test (Figure 5c). There was an additive increase in both SOC decomposition and C efflux, and thus the proportion of C efflux made up of decomposed SOC declined from 41% to 31%. In both the C- and C and N-addition scenarios, a greater proportion of the enhanced C efflux was derived from added C rather than native SOC. There was a small accumulation (3–4 gC m^{-2}) of SOC in the C- and C and N-addition scenarios. This SOC had a C:N of 9.9 and 7.4, respectively, indicating that microbial biomass turnover contributed to soil carbon accumulation (Table 3). In the N-addition scenario, there was an SOC loss of 1.9 gC m^{-2} over the 95 day addition. The magnitude of SOC change in any of the three scenarios would be undetectable in the field using soil sampling methods [*Fahey et al.*, 2005] and insignificant relative to estimates of soil C sinks for the site [*Gaudinski et al.*, 2000].

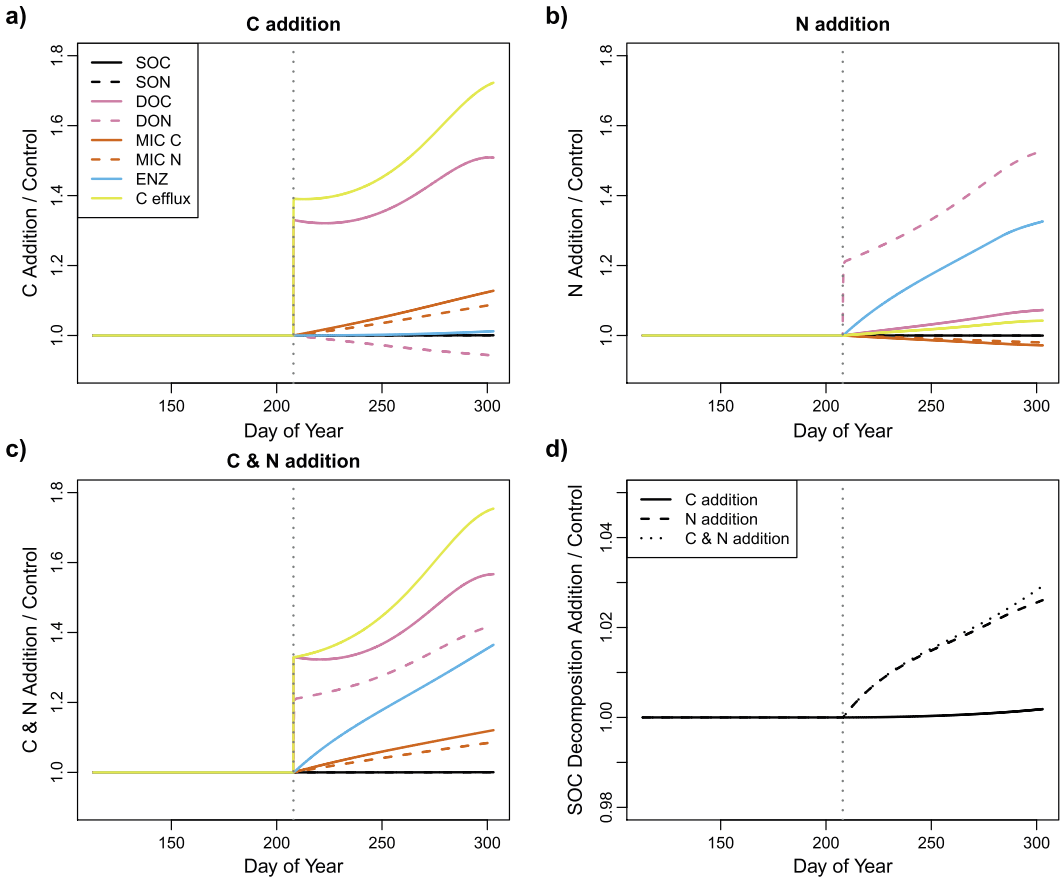

Figure 5. Times series of C and N pools and C efflux rate under (a) C addition, (b) N addition, and (c) C and N addition. (d) C decomposition per unit microbial biomass is plotted for all three addition scenarios. In all plots, the pool sizes and efflux rate were normalized by dividing by the respective pool size or efflux rate in the control run. The gray vertical dotted line marks the beginning of the addition experiment. When dashed lines are not visible, they are overlaying the solid line of the same color (e.g., microbial biomass C and N increase at the same rate). MIC C, MIC N, and ENZ refer to microbial biomass C, microbial biomass N, and enzyme pool size, respectively.

4. Discussion

We have developed a C- and N-explicit model with a theoretical foundation of microbial physiological principles. We did this by building up from the mechanistic DAMM model of enzyme kinetics based on substrate supply [*Davidson et al.*, 2012]. The combined model, DAMM-MCNiP, is unique in that it combines Arrhenius temperature sensitivity, a simple diffusion approximation, stoichiometric constraints, and enzyme-mediated decomposition of SOM and represents these processes with relatively low parameter collinearity. It is therefore a useful tool for examining interactions between microbes and environmental forcings. Unlike soil decomposition models used in most terrestrial biosphere models for the past 40 years, which do not include explicit feedbacks between microbes and the environment [*Parton et al.*, 1987; *Jenkinson and Coleman*, 2008], the DAMM-MCNiP model can generate hypotheses for a variety of measurable C and N pools and fluxes as they affect microbial production of enzymes that depolymerize SOC. Below we will discuss controls on decomposition in DAMM-MCNiP, model performance, hysteresis, priming, limitations, and the utility of modeling coupled C and N cycling.

Table 3. In a 95 Day Model Simulation of DAMM-MCNiP, the Change in SOC Pool Size and C:N of the SOC That Either Accumulated or Depleted Under C Addition, N Addition, and C and N Addition

	Change in SOC Pool (gC m^{-2})	C:N of ΔSOM
C addition	4.0	9.9
N addition	−1.9	17.6
C and N addition	3.4	7.4

4.1. Model Performance

In DAMM-MCNiP temperature and soil moisture affect C efflux and SOC

in predictable ways. Warming consistently increased C efflux and depleted SOC, while drought lowered C efflux and increased SOC. Of course, prolonged drought would likely decrease plant productivity and litter inputs over the long term, thus reversing initial gains in SOC, but such ecosystem level interactions are not included in this soil model.

The seasonality of the temperature and moisture forcings in DAMM-MCNiP affected the C efflux rate in different ways. Although soil temperature was more tightly correlated with C efflux than was soil moisture (Table 2), soil moisture provided important information about the variability of C efflux on short temporal scales (Figure S3) and was better correlated with C efflux during wet-up events. This result is consistent with higher statistical correlation between soil respiration and soil temperature at seasonal time scales but higher correlation with soil moisture at short-time scales on the order of days, which are more characteristic of synoptic weather patterns [*Savage et al*., 2009]. In DAMM, soil moisture modifies only the decomposition rate, but in DAMM-MCNiP it directly modifies decomposition and microbial uptake and indirectly modifies other downstream microbial processes (e.g., enzyme production, biomass growth). As a result, the combination of DAMM with MCNiP in the present study resulted in a larger stimulation of C efflux following precipitation events compared to DAMM alone (Table 2).

Microbial activity may also vary seasonally in ways that are not directly related to temperature or soil moisture. *Drake et al*. [2013] found support for seasonal plasticity in the temperature sensitivity of a number of processes modeled here such as microbial respiration, enzyme activity, and N mineralization. Temperature hysteresis in soil respiration is a well-documented example of this that can be attributed to the timing of plant inputs [*Oikawa et al*., 2014; *Zhang et al*., 2015] and influenced by feedbacks to microbial activity [*Bradford et al*., 2008]. In the model, substrate limitation early in the growing season (DOY ~115, Figure S6c) suppressed C efflux relative to soil at the same temperature in the late fall (DOY ~280, Figure 3). By the midgrowing season, however (DOY 150–200, Figure 3), substrate limitation was alleviated (Figure S6c). As a result, high enzyme production and microbial biomass growth produced higher rates of C efflux than those measured at the same temperature in the midfall (DOY 220–270, Figure 3) when DOC again declined, resulting in a lagged decrease in microbial biomass and enzyme production (Figures S6b–S6d). The temperature hysteresis observed in the field cannot be explained by the DAMM and Arrhenius models nor by a simple two-pool soil model (Figures S8a and S8b and Text S4) [*Kelly et al*., 2000; *Davidson et al*., 2012; *Sierra et al*., 2012]. However, the observed hysteresis is consistent with that generated by DAMM-MCNiP (Figure 3). DAMM-MCNiP's consistency with the observed hysteresis can be weakened by removing the seasonality of plant inputs (Figure S8d), suggesting that seasonal variations in substrate supply controlled by biotic processes (i.e., plant inputs and subsequent enzyme production and depolymerization) are as important as physical factors (e.g., soil temperature and moisture) in explaining seasonal-scale variation in microbial respiration.

4.2. Temperature Sensitivity of Decomposition

The sensitivity analysis identified the activation energy of decomposition as the most important parameter for predicting the C efflux rate across the seasonal measurement period at the Harvard Forest study site. Parameter fitting to C efflux data suggests that the value of Ea_{dep} is 64 kJ mol^{-1}. This value is at the upper end of the range of activation energies estimated by *Davidson et al*. [2012] using laboratory-based assays of β-glucosidase activity ($Ea_{dep} \approx$ 59–64 kJ mol^{-1}) but well within the range reported for forest soil in other studies (63–84 kJ mol^{-1}) [*Yvon-durocher et al*., 2012; *Fang and Moncrieff*, 2001]. Although organic matter decomposition is carried out by a wide variety of extracellular enzymes, β-glucosidase has higher activity than other commonly measured enzymes across many biomes [*Steinweg et al*., 2013]. Small changes in the activation energy parameter have a large effect on C efflux rate in most models based on Arrhenius kinetics because of the exponential relationship between rate and activation energy [*Schipper et al*., 2014], suggesting that measurements of β-glucosidase activity and other soil enzymes may be important for constraining process models of soil decomposition. Activation energy modifies the temperature sensitivity of C efflux, suggesting that temperature is the most important environmental factor determining C efflux when considering variation from spring to autumn at this site [*Flanagan and Johnson*, 2005; *Sinsabaugh et al*., 2017]. Processes other than C efflux, such as N mineralization or microbial biomass growth, may be more sensitive to different inputs and parameters but are beyond the scope of the present study.

4.3. Plant Input Addition

The stoichiometry of plant inputs determined the proportion of C efflux from native SOC in our idealized C- and N-addition scenarios. The C- and C and N-addition scenarios caused a 40–80% increase in C efflux, which is commonly observed in field and laboratory priming experiments [*Hamer and Marschner*, 2005; *Dijkstra and Cheng*, 2007a; *Drake et al*., 2013; *Han et al*., 2015]. In our model scenario adding high C:N substrate, microbes preferentially utilized the added substrate rather than decomposing native SOC, resulting in a suppression of SOC decomposition relative to the control. The C:N of the small increase in SOC indicated that it was of microbial origin, reflecting the contribution of microbial biomass turnover (C addition) or both microbial biomass and enzyme turnover (C and N addition).

In the N-addition scenario, production of N-rich enzymes stimulated SOC decomposition resulting in a "real" priming effect in the sense of *Kuzyakov* [2010]. This priming effect was accompanied by greater N mineralization (Figure S9). *Drake et al*. [2013] also found that adding N-rich substrate supported enzyme production and resulted in greater N mineralized as a result of SOC decomposition. DAMM-MCNiP predicted a small initial stimulation of soil CO_2 flux after N addition, which was a similar response to some experimental additions of N at the Harvard Forest. These N-addition experiments observed either a modest short-term increase in CO_2 flux or no change [*Micks et al*., 2004; *Contosta et al*., 2011]. DAMM-MCNiP provides a mechanistic framework for evaluating that response. Additional N allowed a pulse of enzyme production that stimulated depolymerization, but released DOC was inadequate to grow microbial biomass C relative to the control. The opposite was true under C addition: microbial biomass growth was supported, but there was not enough N to produce enzymes. Microbes may alleviate N limitation under C addition by shifting allocation from biomass growth to enzymes, or by shifting allocation to enzymes that degrade N-rich as opposed to C-rich substrates, but DAMM-MCNiP does not currently support multiple enzymes. Further, microbial immobilization of inorganic N may alleviate N limitation, and competition with mineral surfaces and plants for N could also affect N dynamics [*Zhu et al*., 2016]. Substrate-specific enzymes and inorganic N cycling would be logical follow-on areas of model development that could be useful for posing further hypotheses about coupled C and N cycling.

A CO_2 enrichment experiment in North Carolina measured an increase in soil respiration, microbial biomass, and SOC with increasing plant C inputs [*Drake et al*., 2011]. Our model results are consistent with these findings indicating that C addition supports a larger microbial biomass whose turnover and processing of litter contributes to faster rates of soil respiration. The extent to which SOM accumulated depended on the C:N of inputs. Because enzymes (C:N = 3) require more N than microbial biomass (C:N = 10), the N content of the inputs determined whether microbes produced relatively more enzymes or biomass. This partitioning determined the balance between SOC loss via enzymatic decomposition, and accumulation via enzyme and microbial turnover. Variation in the stoichiometry of inputs may contribute to the large variation in both sign and magnitude of change across plant input experiments [*Dijkstra and Cheng*, 2007b; *Drake et al*., 2011; *Lajtha et al*., 2014; *Zhu et al*., 2014; *Pisani et al*., 2015].

4.4. Conclusions

We have developed a model, DAMM-MCNiP, that is parsimonious, in terms of model inputs and ease of parameter fitting, and modular in that it can be broken down into its simpler component models (DAMM and MCNiP) if desired. Though there is a growing number of microbial models with explicit C-N linkages (Table S1) [*Allison*, 2005; *Fontaine and Barot*, 2005; *Kaiser et al*., 2014; *Moorhead et al*., 2012; *Waring et al*., 2013], none that we know of represents temperature, soil moisture, and nitrogen effects together. DAMM-MCNiP includes the simplest mechanistic representation of these drivers based on enzyme kinetics, diffusion, and stoichiometry. In particular, the relatively low collinearity of the combined model minimizes concerns about equifinality commonly raised for more complex models. Further, DAMM-MCNiP features more robust decomposition kinetics than that in most soil decomposition models, requiring fewer assumptions to maintain mass balance [*Tang*, 2015].

DAMM-MCNiP could be used to examine the microbial processes underlying observable phenomena, such as seasonal hystereses in respiration rates or priming as a function of substrate stoichiometry. It can simulate rhizosphere and bulk soil and could be scaled using diffusive transport principles (in the sense of *Ahrens et al*. [2015] and *Tang et al*. [2013]) to represent rhizosphere bulk or surface depth gradients explicitly.

DAMM-MCNiP can be used to project C and N cycling at the site level, using field experiments that measure C efflux in combination with periodic sampling of soil pools or incubation experiments that target microbial and enzyme activity in response to changes in temperature or substrate supply. Here we used DAMM-MCNiP to demonstrate that seasonality in substrate supply and consequent microbial activity explains an observed temperature hysteresis and that microbial response to substrate stoichiometry can theoretically explain the variation in priming responses observed after plant input manipulations.

Acknowledgments
This research was supported by the U.S. Department of Energy, grants DE-SC0006916, DE-SC0012288, and DE-AC02-05CH11231; the National Science Foundation (DEB 1237491); U.S. Department of Agriculture grant 2014-67003-22073; and the American Association of University Women Doctoral Dissertation Fellowship. The DAMM-MCNiP code developed in this manuscript is archived and publicly accessible in a GitHub repository: https://github.com/rabramoff/DAMM-MCNiPv0. The C efflux measurements used in this study and related metadata can be accessed at the Harvard Forest Data Archive, a freely accessible online archive of measurements made at the Harvard Forest Long Term Ecological Research Site. The URL for the archive is: http://harvardforest.fas.harvard.edu/harvard-forest-data-archive, and the ID for the data set is HF243-01.

References

Abramoff, R., and A. Finzi (2016), Seasonality and partitioning of root allocation to rhizosphere soils in a mid-latitude forest, *Ecosphere*, *7*, e01547, doi:10.1002/ecs2.1547.

Ahrens, B., M. C. Braakhekke, G. Guggenberger, M. Schrumpf, and M. Reichstein (2015), Contribution of sorption, DOC transport and microbial interactions to the ^{14}C age of a soil organic carbon profile: Insights from a calibrated process model, *Soil Biol. Biochem.*, *88*, 390–402, doi:10.1016/j.soilbio.2015.06.008.

Allison, S. D. (2005), Cheaters, diffusion and nutrients constrain decomposition by microbial enzymes in spatially structured environments, *Ecol. Lett.*, *8*(6), 626–635, doi:10.1111/j.1461-0248.2005.00756.x.

Allison, S. D., M. D. Wallenstein, and M. A. Bradford (2010), Soil-carbon response to warming dependent on microbial physiology, *Nat. Geosci.*, *3*(5), 336–340, doi:10.1038/ngeo846.

Arrhenius, S. (1889a), Über die Dissociationswärme und den Einfluss der Temperatur auf den Dissociationsgrad der Elektrolyte, *Z. Phys. Chem.*, *4*(1), 96–116.

Arrhenius, S. (1889b), Über die Reaktionsgeschwindigkeit bei der Inversion von Rohrzucker durch Säuren, *Z. Phys. Chem.*, *4*(1), 226–248.

Averill, C. (2014), Divergence in plant and microbial allocation strategies explains continental patterns in microbial allocation and biogeochemical fluxes, *Ecol. Lett.*, *17*(10), 1202–1210, doi:10.1111/ele.12324.

Birch, H. F. (1958), The effect of soil drying on humus decomposition and nitrogen availability, *Plant Soil*, *10*(1), 9–31.

Bolker, B. M., S. W. Pacala, and W. J. Parton (1998), Linear analysis of soil decomposition: Insights from the century model, *Ecol. Appl.*, *8*(2), 425–439.

Boose, E., and M. VanScoy (2015), Fisher Meteorological Station at Harvard Forest since 2001, Retrieved from Harvard For. Data Arch. (HF001) Harvard Forest, Petersham, Mass. [Available at http://harvardforest.fas.harvard.edu:8080/exist/apps/datasets/showData.html?id=hf001.]

Bradford, M. A., C. A. Davies, S. D. Frey, T. R. Maddox, J. M. Melillo, J. E. Mohan, J. F. Reynolds, K. K. Treseder, and M. D. Wallenstein (2008), Thermal adaptation of soil microbial respiration to elevated temperature, *Ecol. Lett.*, *11*(12), 1316–1327, doi:10.1111/j.1461-0248.2008.01251.x.

Brun, R., P. Reichert, and H. R. Kunsch (2001), Practical identifiability analysis of large environmental simulation models, *Water Resour. Res.*, *37*(4), 1015–1030, doi:10.1029/2000WR900350.

Brzostek, E., and A. Finzi (2011), Substrate supply, fine roots, and temperature control proteolytic enzyme activity in temperate forest soils, *Ecology*, *92*(4), 892–902.

Brzostek, E. R., A. Greco, J. E. Drake, and A. C. Finzi (2013), Root carbon inputs to the rhizosphere stimulate extracellular enzyme activity and increase nitrogen availability in temperate forest soils, *Biogeochemistry*, *115*(1–3), 65–76, doi:10.1007/s10533-012-9818-9.

Cleveland, C. C., and D. Liptzin (2007), C:N:P stoichiometry in soil: Is there a "Redfield ratio" for the microbial biomass?, *Biogeochemistry*, *85*, 235–252, doi:10.1007/s10533-007-9132-0.

Coleman, K., and D. S. Jenkinson (1996), RothC-26.3 - A model for the turnover of carbon in soil, in *Evaluation of Soil Organic Matter Models*, pp. 237–246.

Contosta, A. R., S. D. Frey, and A. B. Cooper (2011), Seasonal dynamics of soil respiration and N mineralization in chronically warmed and fertilized soils, *Ecosphere*, *2*(3), 1–17, doi:10.1890/ES10-00133.1.

Davidson, E. A., S. Samanta, S. S. Caramori, and K. Savage (2012), The dual Arrhenius and Michaelis–Menten kinetics model for decomposition of soil organic matter at hourly to seasonal time scales, *Global Change Biol.*, *18*(1), 371–384.

Davidson, E. A., K. E. Savage, and A. C. Finzi (2014), A big-microsite framework for soil carbon modeling, *Global Change Biol.*, *20*(12), 3610–3620.

Dijkstra, F., and W. Cheng (2007a), Moisture modulates rhizosphere effects on C decomposition in two different soil types, *Soil Biol. Biochem.*, *39*, 2264–2274, doi:10.1016/j.soilbio.2007.03.026.

Dijkstra, F. A., and W. Cheng (2007b), Interactions between soil and tree roots accelerate long-term soil carbon decomposition, *Ecol. Lett.*, *10*(11), 1046–1053, doi:10.1111/j.1461-0248.2007.01095.x.

Drake, J. E., et al. (2011), Increases in the flux of carbon belowground stimulate nitrogen uptake and sustain the long-term enhancement of forest productivity under elevated CO_2, *Ecol. Lett.*, *14*(4), 349–357, doi:10.1111/j.1461-0248.2011.01593.x.

Drake, J. E., B. A. Darby, M.-A. Giasson, M. A. Kramer, R. P. Phillips, and A. C. Finzi (2013), Stoichiometry constrains microbial response to root exudation—Insights from a model and a field experiment in a temperate forest, *Biogeosciences*, *10*(2), 821–838, doi:10.5194/bg-10-821-2013.

Epron, D., L. Farque, E. Lucot, and P.-M. Badot (1999), Efflux in a beech forest: The contribution of root respiration, *Ann. For. Sci.*, *56*(4), 289–295, doi:10.1051/forest:19990403.

Fahey, T. J., et al. (2005), The biogeochemistry of carbon at Hubbard Brook, *Biogeochemistry*, *75*(1), 109–176, doi:10.1007/s10533-004-6321-y.

Fang, C., and J. B. Moncrieff (2001), The dependence of soil CO_2 efflux on temperature, *Soil Biol. Biochem.*, *33*, 155–165.

Farrar, J., M. Hawes, D. Jones, and S. Lindow (2003), How roots control the flux of carbon to the rhizosphere, *Ecology*, *84*(4), 827–837.

Finzi, A. C., A. T. Austin, E. E. Cleland, S. D. Frey, B. Z. Houlton, and M. D. Wallenstein (2011), Responses and feedbacks of coupled biogeochemical cycles to climate change: Examples from terrestrial ecosystems, *Front. Ecol. Environ.*, *9*(1), 61–67.

Finzi, A. C., R. Z. Abramoff, K. S. Spiller, E. R. Brzostek, B. A. Darby, M. A. Kramer, and R. P. Phillips (2015), Rhizosphere processes are quantitatively important components of terrestrial carbon and nutrient cycles, *Global Change Biol.*, *21*(5), 2082–2094.

Flanagan, L. B., and B. G. Johnson (2005), Interacting effects of temperature, soil moisture and plant biomass production on ecosystem respiration in a northern temperate grassland, *Agric. For. Meteorol.*, *130*, 237–253, doi:10.1016/j.agrformet.2005.04.002.

Fontaine, S., and S. Barot (2005), Size and functional diversity of microbe populations control plant persistence and long-term soil carbon accumulation, *Ecol. Lett.*, *8*(10), 1075–1087, doi:10.1111/j.1461-0248.2005.00813.x.

Fontaine, S., G. Bardoux, L. Abbadie, and A. Mariotti (2004), Carbon input to soil may decrease soil carbon content, *Ecol. Lett.*, *7*, 314–320, doi:10.1111/j.1461-0248.2004.00579.x.

Frey, S. D., J. Lee, J. M. Melillo, and J. Six (2013), The temperature response of soil microbial efficiency and its feedback to climate, *Nat. Clim. Change*, *3*(4), 395–398, doi:10.1038/nclimate1796.

Gaudinski, J. B., S. E. Trumbore, A. Eric, and S. Zheng (2000), Soil carbon cycling in a temperate forest: Radiocarbon-based estimates of residence times, sequestration rates and partitioning of fluxes, *Biogeochemistry*, *51*, 33–69.

German, D. P., K. R. B. Marcelo, M. M. Stone, and S. D. Allison (2012), The Michaelis-Menten kinetics of soil extracellular enzymes in response to temperature: A cross-latitudinal study, *Global Change Biol.*, *18*(4), 1468–1479, doi:10.1111/j.1365-2486.2011.02615.x.

Giasson, M.-A., et al. (2013), Soil respiration in a northeastern US temperate forest: A 22-year synthesis, *Ecosphere*, *4*, 1–28, doi:10.1890/ES13.00183.1.

Graaff, M., A. De, T. Classen, H. F. Castro, and C. W. Schadt (2010), Labile soil carbon inputs mediate the soil microbial community composition and plant residue decomposition rates, *New Phytol.*, *188*, 1055–1064, doi:10.1111/j.1469-8137.2010.03427.x.

Grant, R. F., N. G. Juma, and W. B. McGill (1993), Simulation of carbon and nitrogen transformations in soil: Microbial biomass and metabolic products, *Soil Biol. Biochem.*, *25*(10), 1331–1338, doi:10.1016/0038-0717(93)90047-F.

Hamer, U., and B. Marschner (2005), Priming effects in soils after combined and repeated substrate additions, *Geoderma*, *128*, 38–51, doi:10.1016/j.geoderma.2004.12.014.

Han, T., W. Huang, J. Liu, G. Zhou, and Y. Xiao (2015), Different soil respiration responses to litter manipulation in three subtropical successional forests, *Sci Rep.*, *5*, 18166.

Hararuk, O., M. J. Smith, and Y. Luo (2015), Microbial models with data-driven parameters predict stronger soil carbon responses to climate change, *Global Change Biol.*, *21*(6), 2439–2453, doi:10.1111/gcb.12827.

Hartley, I. P., M. Garnett, M. Sommerkorn, D. W. Hopkins, B. J. Fletcher, V. L. Sloan, G. K. Phoenix, and P. A. Wookey (2012), A potential loss of carbon associated with greater plant growth in the European Arctic, *Nat. Clim. Change*, *2*(12), 875–879, doi:10.1038/nclimate1575.

He, Y., J. Yang, Q. Zhuang, J. W. Harden, A. D. McGuire, Y. Liu, G. Wang, and L. Gu (2015), Incorporating microbial dormancy dynamics into soil decomposition models to improve quantification of soil carbon dynamics of northern temperate forests, *J. Geophys. Res. Biogeosci.*, *120*, 2596–2611, doi:10.1002/2015JG003130.

Högberg, P., A. Nordgren, N. Buchmann, A. F. Taylor, A. Ekblad, M. N. Högberg, G. Nyberg, M. Ottosson-Löfvenius, and D. J. Read (2001), Large-scale forest girdling shows that current photosynthesis drives soil respiration, *Nature*, *411*(6839), 789–792, doi:10.1038/35081058.

Hopkinson, C. S., B. Fry, and A. L. Nolin (1997), Stoichiometry of dissolved organic matter dynamics on the continental shelf of the northeastern USA, *Cont. Shelf Res.*, *17*(5), 473–489.

Jenkinson, D. S., and K. Coleman (2008), The turnover of organic carbon in subsoils. Part 2. Modelling carbon turnover, *Eur. J. Soil Sci.*, *59*(2), 400–413.

Jenkinson, D. S., S. P. S. Andrew, J. M. Lynch, M. J. Goss, and P. B. Tinker (1990), The turnover of organic carbon and nitrogen in soil [and discussion], *Philos. Trans. R. Soc. London Ser. B Biol. Sci.*, *329*(1255), 361–368.

Kaiser, C., O. Franklin, U. Dieckmann, and A. Richter (2014), Microbial community dynamics alleviate stoichiometric constraints during litter decay, *Ecol. Lett.*, *17*(6), 680–690, doi:10.1111/ele.12269.

Keiluweit, M., J. J. Bougoure, P. S. Nico, J. Pett-Ridge, P. K. Weber, and M. Kleber (2015), Mineral protection of soil carbon counteracted by root exudates, *Nat. Clim. Change*, *5*(6), 588–595, doi:10.1038/nclimate2580.

Kelly, R., W. Parton, M. Hartman, L. Stretch, D. Ojima, and D. Schimel (2000), Intra-annual and interannual variability of ecosystem processes in a shortgrass steppe, *J. Geophys. Res.*, *105*(D15), 20093–20100.

Kuzyakov, Y. (2010), Priming effects: Interactions between living and dead organic matter, *Soil Biol. Biochem.*, *42*(9), 1363–1371, doi:10.1016/j.soilbio.2010.04.003.

Lajtha, K., K. L. Townsend, M. G. Kramer, C. Swanston, R. D. Bowden, and K. Nadelhoffer (2014), Changes to particulate versus mineral-associated soil carbon after 50 years of litter manipulation in forest and prairie experimental ecosystems, *Biogeochemistry*, *119*(1–3), 341–360, doi:10.1007/s10533-014-9970-5.

Lawrence, C. R., J. C. Neff, and J. P. Schimel (2009), Does adding microbial mechanisms of decomposition improve soil organic matter models? A comparison of four models using data from a pulsed rewetting experiment, *Soil Biol. Biochem.*, *41*(9), 1923–1934, doi:10.1016/j.soilbio.2009.06.016.

Lemos, P. (2013), Variations in carbon fluxes lead to resilience of carbon storage in New England forests affected by the hemlock woolly adelgid at a centennial time scale, PhD thesis, Boston Univ., Boston, Mass. [Available at http://hdl.handle.net/2144/13122l.]

Lloyd, J., and J. A. Taylor (1994), On the temperature dependence of soil respiration, *Funct. Ecol.*, *8*(3), 315–323.

Magill, A. H., J. D. Aber, G. M. Berntson, W. H. McDowell, K. J. Nadelhoffer, J. M. Melillo, and P. Steudler (2000), Long-term nitrogen additions and nitrogen saturation in two temperate forests, *Ecosystems*, *3*(3), 238–253.

Manzoni, S., and A. Porporato (2009), Soil carbon and nitrogen mineralization: Theory and models across scales, *Soil Biol. Biochem.*, *41*(7), 1355–1379, doi:10.1016/j.soilbio.2009.02.031.

Manzoni, S., S. M. Schaeffer, G. Katul, A. Porporato, and J. P. Schimel (2014), A theoretical analysis of microbial eco-physiological and diffusion limitations to carbon cycling in drying soils, *Soil Biol. Biochem.*, *73*(0), 69–83, doi:10.1016/j.soilbio.2014.02.008.

Matlab version 8.6.0. (2017), The MathWorks Inc., Natick, Mass.

McGroddy, M. E., T. Daufresne, and L. O. Hedin (2004), Scaling of C:N:P stoichiometry in forests worldwide: Implications of terrestrial redfield-type ratios, *Ecology*, *85*(9), 2390–2401.

Micks, P., J. D. Aber, R. D. Boone, and E. A. Davidson (2004), Short-term soil respiration and nitrogen immobilization response to nitrogen applications in control and nitrogen-enriched temperate forests, *For. Ecol. Manage*, *196*(1), 57–70.

Moorcroft, P. R., G. C. Hurtt, and S. W. Pacala (2001), A method for scaling vegetation dynamics: The ecosystem demography model (ED), *Ecol. Monogr.*, *71*(4), 557–586, doi:10.1890/0012-9615(2001)071[0557:AMFSVD]2.0.CO;2.

Moorhead, D. L., and R. L. Sinsabaugh (2006), A theoretical model of litter decay and microbial interaction, *Ecol. Monogr.*, *76*(2), 151–174.

Moorhead, D. L., G. Lashermes, and R. L. Sinsabaugh (2012), A theoretical model of C- and N-acquiring exoenzyme activities, which balances microbial demands during decomposition, *Soil Biol. Biochem.*, *53*, 133–141, doi:10.1016/j.soilbio.2012.05.011.

Mooshammer, M., et al. (2014), Adjustment of microbial nitrogen use efficiency to carbon:nitrogen imbalances regulates soil nitrogen cycling, *Nat. Commun.*, *5*, 3694, doi:10.1038/ncomms4694.

Munger, W., J. L. Hadley, M. VanScoy, and L. Nicoll (2016), Microclimate at Harvard Forest HEM, LPH and EMS Towers since 2005, Retrieved from Harvard For. Data Arch. (HF206) Harvard Forest, Petersham, Mass. [Available at http://harvardforest.fas.harvard.edu:8080/exist/apps/datasets/showData.html?id=hf206.]

Murphy, C. J., E. M. Baggs, N. Morley, D. P. Wall, and E. Paterson (2015), Rhizosphere priming can promote mobilisation of N-rich compounds from soil organic matter, *Soil Biol. Biochem.*, *81*, 236–243, doi:10.1016/j.soilbio.2014.11.027.

Neff, J. C., and D. U. Hooper (2002), Vegetation and climate controls on potential CO_2, DOC and DON production in northern latitude soils, *Global Change Biol.*, *8*(9), 872–884.

Oikawa, P. Y., D. A. Grantz, A. Chatterjee, J. E. Eberwein, L. A. Allsman, and G. D. Jenerette (2014), Unifying soil respiration pulses, inhibition, and temperature hysteresis through dynamics of labile soil carbon and O_2, *J. Geophys. Res. Biogeosci.*, *119*, 521–536, doi:10.1002/2013JG002434.

Omlin, M., R. Brun, and P. Reichert (2001), Biogeochemical model of Lake Zu sensitivity, identifiability and uncertainty analysis, *Ecol. Model.*, *141*, 105–123.

Parton, W. J., D. S. Schimel, C. V. Cole, D. S. Oiima, and D. S. Ojima (1987), Analysis of factors controlling soil organic matter levels in Great Plains grasslands, *Soil Sci. Soc. Am. J.*, *51*(i), 1173–1179.

Pianosi, F., F. Sarrazin, and T. Wagener (2015), A Matlab toolbox for Global Sensitivity Analysis, *Environ. Modell. Softw.*, *70*, 80–85, doi:10.1016/j.envsoft.2015.04.009.

Pisani, O., L. H. Lin, O. O. Y. Lun, K. Lajtha, K. J. Nadelhoffer, A. J. Simpson, and M. J. Simpson (2015), Long-term doubling of litter inputs accelerates soil organic matter degradation and reduces soil carbon stocks, *Biogeochemistry*, *127*(1), 1–14, doi:10.1007/s10533-015-0171-7.

Rodrigo, A., S. Recous, C. Neel, and B. Mary (1997), Modelling temperature and moisture effects on C-N transformations in soils: Comparison of nine models, *Ecol. Model.*, *102*(2–3), 325–339, doi:10.1016/S0304-3800(97)00067-7.

Saltelli, A., M. Ratto, T. Andres, F. Campolongo, J. Cariboni, D. Gatelli, M. Saisana, and S. Tarantola (2008), Global sensitivity analysis, the primer, *Int. Stat. Rev.*, *76*(3), 452.

Saltelli, A., P. Annoni, I. Azzini, F. Campolongo, M. Ratto, and S. Tarantola (2010), Variance based sensitivity analysis of model output. Design and estimator for the total sensitivity index, *Comput. Phys. Commun.*, *181*(2), 259–270.

Savage, K., E. A. Davidson, A. D. Richardson, and D. Y. Hollinger (2009), Three scales of temporal resolution from automated soil respiration measurements, *Agric. For. Meteorol.*, *149*(11), 2012–2021, doi:10.1016/j.agrformet.2009.07.008.

Savage, K., E. A. Davidson, and J. Tang (2013), Diel patterns of autotrophic and heterotrophic respiration among phenological stages, *Global Change Biol.*, *19*(4), 1151–1159, doi:10.1111/gcb.12108.

Schimel, J. P., and M. N. Weintraub (2003), The implications of exoenzyme activity on microbial carbon and nitrogen limitation in soil: A theoretical model, *Soil Biol. Biochem.*, *35*(4), 549–563, doi:10.1016/S0038-0717(03)00015-4.

Schipper, L. A., J. K. Hobbs, S. Rutledge, and V. L. Arcus (2014), Thermodynamic theory explains the temperature optima of soil microbial processes and high Q10 values at low temperatures, *Global Change Biol.*, *20*(11), 3578–3586, doi:10.1111/gcb.12596.

Schlesinger, W. H. (2005), *Biogeochemistry*, Gulf Professional Publishing, Oxford, U. K.

Schlesinger, W. H., and E. S. Bernhardt (2013), *Biogeochemistry: An Analysis of Global Change*, 3rd ed., Academic Press Elsevier, Waltham, Mass., and Oxford, U. K.

Schuur, E. A., and S. E. Trumbore (2006), Partitioning sources of soil respiration in boreal black spruce forest using radiocarbon, *Glob. Chang. Biol.*, *12*, 165–176, doi:10.1111/j.1365-2486.2005.01066.x.

Shevliakova, E., S. W. Pacala, S. Malyshev, G. C. Hurtt, P. C. D. Milly, J. P. Caspersen, L. T. Sentman, J. P. Fisk, C. Wirth, and C. Crevoisier (2009), Carbon cycling under 300 years of land use change: Importance of the secondary vegetation sink, *Global Biogeochem. Cycles*, *23*, GB2022, doi:10.1029/2007GB003176.

Sierra, C. A., M. Müller, and S. E. Trumbore (2012), Models of soil organic matter decomposition: The SoilR package, version 1.0, *Geosci. Model Dev.*, *5*(4), 1045–1060, doi:10.5194/gmd-5-1045-2012.

Sierra, C. A., S. E. Trumbore, E. A. Davidson, S. Vicca, and I. Janssens (2015), Sensitivity of decomposition rates of soil organic matter with respect to simultaneous changes in temperature and moisture, *J. Adv. Model. Earth Syst.*, *7*, 335–356, doi:10.1002/2014MS000358.

Sinsabaugh, R. L., D. L. Moorhead, X. Xu, and M. E. Litvak (2017), Plant, microbial and ecosystem carbon use efficiencies interact to stabilize microbial growth as a fraction of gross primary production, *New Phytol.*, *214*(4), 1518–1526, doi:10.1111/nph.14485.

Sistla, S. A., E. B. Rastetter, and J. P. Schimel (2014), Responses of a tundra system to warming using SCAMPS: A stoichiometrically coupled, acclimating microbe–plant–soil model, *Ecol. Monogr.*, *84*(1), 151–170.

Soetaert, K. (2016), R Package FME: Inverse modelling, sensitivity, Monte Carlo—Applied to a dynamic simulation model, (CRAN Vignette 2). [Availavle at https://cran.r-project.org/web/packages/FME/vignettes/FMEdyna.pdf.]

Stanford, G., and E. Epstein (1974), Nitrogen mineralization-water relations in soils, *Soil Sci. Soc. Am. J.*, *38*(1), 103–107.

Stanford, G., M. H. Frere, and D. H. Schwaninger (1973), Temperature coefficient of soil nitrogen mineralization, *Soil Sci.*, *115*(4), 321–323.

Steinweg, J. M., S. Jagadamma, J. Frerichs, and M. A. Mayes (2013), Activation energy of extracellular enzymes in soils from different biomes, *PLoS One*, *8*(3), e59943, doi:10.1371/journal.pone.0059943.

Sulman, B. N., R. P. Phillips, A. C. Oishi, E. Shevliakova, and S. W. Pacala (2014), Microbe-driven turnover offsets mineral-mediated storage of soil carbon under elevated CO_2, *Nat. Clim. Change*, *4*, 1099–1102, doi:10.1038/NCLIMATE2436.

Tang, J., and W. J. Riley (2015), Weaker soil carbon–climate feedbacks resulting from microbial and abiotic interactions, *Nat. Clim. Change*, *5*, 56–60, doi:10.1038/nclimate2438.

Tang, J. Y. (2015), On the relationships between the Michaelis–Menten kinetics, reverse Michaelis–Menten kinetics, equilibrium chemistry approximation kinetics, and quadratic kinetics, *Geosci. Model Dev.*, *8*, 3823–3835, doi:10.5194/gmd-8-3823-2015.

Tang, J. Y., W. J. Riley, C. D. Koven, and Z. M. Subin (2013), CLM4-BeTR, a generic biogeochemical transport and reaction module for CLM4: Model development, evaluation, and application, *Geosci. Model Dev.*, *6*, 127–140, doi:10.5194/gmd-6-127-2013.

Todd-Brown, K. E., J. T. Randerson, W. M. Post, F. M. Hoffman, C. Tarnocai, E. A. Schuur, and S. D. Allison (2013), Causes of variation in soil carbon simulations from CMIP5 Earth system models and comparison with observations, *Biogeosciences*, *10*(3), 1717–1736.

Wallenstein, M. D., S. McNulty, I. J. Fernandez, J. Boggs, and W. H. Schlesinger (2006), Nitrogen fertilization decreases forest soil fungal and bacterial biomass in three long-term experiments, *For. Ecol. Manage*, *222*(1–3), 459–468, doi:10.1016/j.foreco.2005.11.002.

Wang, G., and W. M. Post (2013), A note on the reverse Michaelis-Menten kinetics, *Soil Biol. Biochem.*, *57*, 946–949, doi:10.1016/j.soilbio.2012.08.028.

Wang, G., W. M. Post, and M. A. Mayes (2013), Development of microbial-enzyme-mediated decomposition model parameters through steady-state and dynamic analyses, *Ecol. Appl.*, *23*(1), 255–272, doi:10.1890/12-0681.1.

Waring, B. G., C. Averill, and C. V. Hawkes (2013), Differences in fungal and bacterial physiology alter soil carbon and nitrogen cycling: Insights from meta-analysis and theoretical models, *Ecol. Lett.*, *16*(7), 887–894, doi:10.1111/ele.12125.

Weintraub, S. R., W. R. Wieder, C. C. Cleveland, and A. R. Townsend (2012), Organic matter inputs shift soil enzyme activity and allocation patterns in a wet tropical forest, *Biogeochemistry*, *114*(1–3), 1–14.

Wieder, W. R., G. B. Bonan, and S. D. Allison (2013), Global soil carbon projections are improved by modelling microbial processes, *Nat. Clim. Change*, *3*(10), 1–7, doi:10.1038/nclimate1951.

Wieder, W. R., A. S. Grandy, C. M. Kallenbach, and G. B. Bonan (2014), Integrating microbial physiology and physio-chemical principles in soils with the MIcrobial-MIneral Carbon Stabilization (MIMICS) model, *Biogeosciences*, *11*(14), 3899–3917, doi:10.5194/bg-11-3899-2014.

Wieder, W. R., A. S. Grandy, C. M. Kallenbach, P. G. Taylor, and G. B. Bonan (2015), Representing life in the Earth system with soil microbial functional traits in the MIMICS model, *Geosci. Model Dev. Discuss.*, *8*(2), 2011–2052, doi:10.5194/gmdd-8-2011-2015.

Wild, B., et al. (2016), Plant-derived compounds stimulate the decomposition of organic matter in arctic permafrost soils, *Sci Rep.*, *6*, 25607, doi:10.1038/srep25607.

Xu, X., J. P. Schimel, P. E. Thornton, X. Song, F. Yuan, and S. Goswami (2014), Substrate and environmental controls on microbial assimilation of soil organic carbon: A framework for Earth system models, *Ecol. Lett.*, *17*(5), 547–555, doi:10.1111/ele.12254.

Yvon-durocher, G., et al. (2012), Reconciling the temperature dependence of respiration across timescales and ecosystem types, *Nature*, *487*, 472–476, doi:10.1038/nature11205.

Zhang, Q., G. G. Katul, R. Oren, E. Daly, S. Manzoni, and D. Yang (2015), The hysteresis response of soil CO_2 concentration and soil respiration to soil temperature, *J. Geophys. Res. Biogeosci.*, *120*, 1605–1618, doi:10.1002/2015JG003047.

Zhu, B., J. L. M. Gutknecht, D. J. Herman, D. C. Keck, M. K. Firestone, and W. Cheng (2014), Rhizosphere priming effects on soil carbon and nitrogen mineralization, *Soil Biol. Biochem.*, *76*, 183–192, doi:10.1016/j.soilbio.2014.04.033.

Zhu, Q., W. J. Riley, J. Tang, and C. D. Koven (2016), Multiple soil nutrient competition between plants, microbes, and mineral surfaces: Model development, parameterization, and example applications in several tropical forests, *Biogeosciences*, *13*(1), 341–363, doi:10.5194/bg-13-341-2016.